Screening of an external magnetic field by spin currents: the infinite U Hubbard model

Jean-Christian Anglès d'Auriac, Benoît Douçot

Classification
Physics Abstracts
71.10—75.20

Screening of an external magnetic field by spin currents: the infinite U Hubbard model

J.C. Anglès d'Auriac and B. Douçot

Centre de Recherches sur les Très Basses Températures, Laboratoire associé à l'Université Joseph Fourier, CNRS, BP 166, 38042 Grenoble Cedex 9, France

(Received 15 July 1992, accepted in final form 18 August 1992)

Résumé. — Le modèle de Hubbard à répulsion infinie est étudié avec un seul trou en présence d'un champ magnétique externe orbital sur des amas finis de différentes géométries. Des résultats de diagonalisations exactes sont présentés pour l'énergie, le spin total et plusieurs fonctions de corrélation de spin. Ils confirment l'idée que le flux appliqué est compensé par le flux fictif provenant d'une configuration de spins non coplanaires. Ce phénomène est aussi bien illustré par une étude variationnelle.

Abstract. — The infinite U Hubbard model with a single hole in the presence of an external orbital magnetic field is studied on a finite cluster for several geometries. Exact diagonalization results for the energy, total spin and several spin correlation functions are presented. They strongly support the idea of the compensation of the applied flux by a flictitious flux induced by a non-coplanar spin background. A variational study also shows evidence of this phenomenon.

The physics of strongly correlated electronic systems, in connectivity with high temperature superconductivity, has been the focus of many recent theoretical investigations. Among these models, the infinite U Hubbard model is the simplest, since it doesn't contain any energy scale and depends only on the electron density. Until recently, the main result for this system was the Nagaoka theorem [1] which states that the ground state for a single hole on a bipartie lattice has the maximum total spin. However, the stability of ferromagnetism in two dimensions has been further investigated by means of exact diagonalizations on finite clusters [2-4], mean field approximation [5, 6], variational wave function with one spin flip [7-9] and high temperature expansions [10]. For more than one hole, some instabilities have been found on finite lattices [2-5], but have been interpreted as finite size effects [11]. It seems rather likely that the fully polarized state is at least locally stable towards a single spin flip for a finite density x of holes up to $x = 0.29$ [9]. But it is not clear that this remains valid at any finite temperature [10]. High temperature expansions suggest that many low lying excited states with arbitrary small magnetization may dominate the magnetic properties at $T \neq 0$.

Part of our present understanding of strong correlations borrows from exact results in one dimension [12], where a decoupling between charge and spin degrees of freedom has been found. In the infinite U limit for a closed ring, eigenstates are classified by the crystal momentum of the associated squeezed spin chain and the k values for the holes [5]. More precisely, a finite crystal momentum in the spin chain shifts the allowed k values and thus plays the role of a fictitious magnetic flux for the orbital motion of the holes. This idea has been the starting point of some mean field approaches which assume that holes move in a twisted spin background [6]. Actually, a full dynamical treatment can be formulated in terms of a gauge theory [13]. This analogy between a spin field and a fictitious magnetic field suggests that the spin configuration is very sensitive to an external orbital field. Intuitively, the spins adjust so that the fictitious field they generate compensates the applied field. This phenomenon has been studied by exact diagonalization [14] and quantum Monte Carlo [15] simulation. The effect of the spin background is, as expected from this picture, to reduce the energy dependence as a function of the external flux. This result is quite interesting, since it suggests that fictitious fluxes can be generated without a significant reduction of the hopping amplitude. Another motivation to study the infinite U Hubbard model for a single hole in an external field is that in the presence of a finite density of holes, and zero external field, it is possible to represent these holes by hard core bosons bound to singular flux tubes [16]. In a mean field type of approximation, the flux tubes are replaced by a uniform average orbital magnetic field. Since these holes are bosonic, their behavior is related to the low lying states of this effective one hole model.

We should stress that for real systems, the external field couples also to the spins *via* the usual Zeeman **B.S** term. For a single hole, this Zeeman term scales with the system size by contrast to the kinetic energy of the hole, which remains finite in the thermodynamical limit. As a result, our model is not realistic. However the main motivation is to study the interplay between charge and spin degrees of freedom.

This paper is dedicated to a numerical study of this problem, using both exact diagonalizations on finite clusters and variational wave functions. More specifically, we consider the infinite U Hubbard model:

$$H = -\sum_{\langle ij\rangle}\sum_{\sigma} \mathrm{e}^{iA_{ij}}(1-n_{i-\sigma})c^{+}_{i\sigma}c_{j\sigma}(1-nj-\sigma)+\mathrm{h.c} \tag{1}$$

where $c^{+}_{i\sigma}$ is an electron creation operator at site i spin components σ. The i, j summation runs over nearest neighbor bonds and the projection operator enforces the non-double-occupancy constraint. The external field is implemented by the phases A_{ij}, which are related to the flux by:

$$\sum_{\substack{\text{oriented}\\ \text{plaquette}}} A_{ij} = 2\pi\frac{\varphi}{\varphi_0} \tag{2}$$

where φ is the flux through the given plaquette and $\varphi_0 = \frac{h}{e}$ is the elementary flux quantum. As usual, the spectrum and all gauge invariant observables are periodic in φ with period φ_0. Two types of geometries have been considered. First a 4×4 square lattice with free boundary condition and second a closed strip of width 2 and legnth 8. These are shown in figure 1. In the case of the internal annulus is identical to the flux φ_e in the external plaquettes, and one for which $\varphi_i = 0$. For the square geometry, we have chosen a uniform flux φ.

We first discuss the result from the exact diagonalizations. The ground energy and first two excited states are shown in figure 2a for the square cluster. As in previous studies, the energy variation is strongly reduced in comparison to the free particle case. We also observe a coincidence between the maxima of $\mathrm{d}E/\mathrm{d}\varphi$ and the minima of level separation for these low

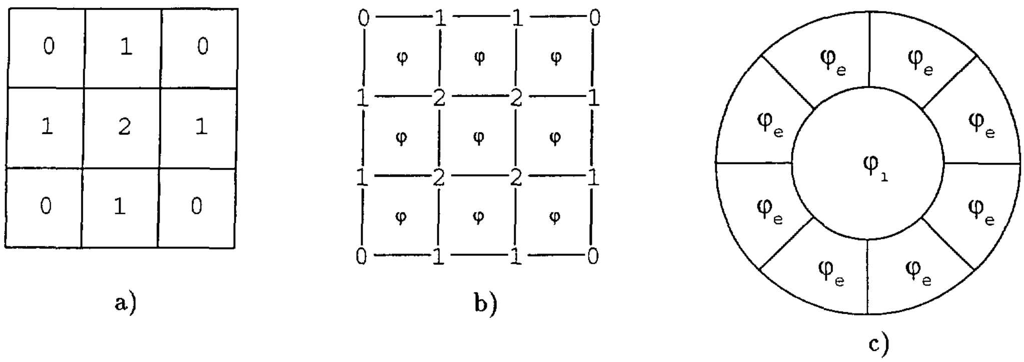

Fig. 1. — Different geometries studied in this work. a) The 4×4 square lattice with open boundary conditions. Numbers on different plaquettes label them according to the symmetries of the cluster. They will be used for figure 5. b) Labels for the different types of sites for the square cluster. They will be used in figure 3. c) The 4×2 strip, with the flux φ_ι for the unique internal plaquette and φ_e for the 8 external plaquettes.

lying states. The same trends are observed for the two ring geometries, suggesting that they are quite general. The total energy variation for the ground state is of the order of 0.02 by contrast to $4 - 2\sqrt{2} \simeq 1.18$ for the infinite square lattice and a single spinless particle. This confirms the picture where spins screen at least partially the applied field by their induced fictitious field. This is strongly supported by further analysis of the ground state wave function. For instance, the probability to find the hole on a given site is depicted in figure 3. As a consequence of the free boundary condition, this probability is reduced for smaller coordination points (ie edges and corners) for the square cluster. For a single spinless particle, it exhibits relatively large fluctuations as a function of the external magnetic field and the discontinuities are due to level crossings. These variations are again reduced by roughly a factor 10 when spin degrees of freedom are included. We note that the characteristic field scale for the oscillations are smaller in the ring geometry that in the square cluster. This is simply a consequence of a larger discretization step for the square cluster. The probability for a spinless particle on a strip to be on the internal annulus ranges from 0.1 to 0.9 when the flux φ is varied. Moreover this probability presents also several discontinuities which are again due to level crossings. The corresponding curves are not shown in figures 3c and 3d because they are off scale.

Another interesting quantity is the total spin *versus* φ. This is plotted in figure 4. We observe that it decreases rather rapidly with φ and reaches its minimum value around $\varphi/\varphi_0 = 0.21$ on the square cluster. This critical φ/φ_0 is 0.11 for the ladder with $\varphi_\iota = 0$ and 0.10 for $\varphi_\iota = \varphi_e$. Note however that in the latter case, the total spin is not a monotonous function of φ. This scale is in quite good agreement with the results of reference [14] and again seems not to depend much on the geometry.

In order to present a more quantitative description of the induced fictitious flux, a good quantity to measure is the expectation value of permutation operators for spins along given closed paths on the lattice. This is related to the fact that when the hole moves along such a closed path, it induces a cyclic permutation of the remaining spins along this path. As usual, the amplitude for such a process has an additional Aharanov-Bohm phase factor $2\pi\ \varphi_{\text{path}}/\varphi_0$ where φ_{path} is the enclosed flux. Perfect screening occurs if spins along the path are in an eigenstate of the associated permutation operator with the eigenvalue $\exp(-i2\pi\ \varphi_{\text{path}}/\varphi_0)$.

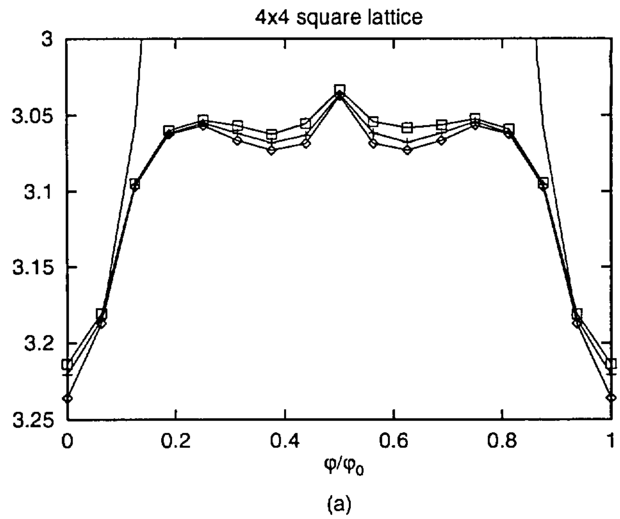

Fig. 2. — Ground state and first excited state energies from exact diagonalization. a) Square cluster with a uniform flux φ per plaquette. The dashed curve is the exact result for a spinless particle (i.e. state with maximal total spin). b) 2×8 strip with $\varphi_{\rm i} = 0$, and $\varphi = \varphi_{\rm e}$. c) 2×8 strip with $\varphi_{\rm i} = \varphi_{\rm e} = \varphi$.

Of course, this cannot be achieved simultaneously for all the paths present in the system. However, on the average, spins may twist in a way which tends to reduce the total phase accumalated by the hole along closed paths. Figure 5 shows the phase of the expectation value of cyclic permutation operators. In figure 5a, the wave function is projected on the subspace where the hole occupies one of the sites of a given plaquette. A cyclic permutation of the three spins on the plaquette is then performed, and the overlap of the final state with the ground state is calculated. The phase of this overlap is denoted by $2\pi\varphi_{\rm fic}/\varphi_0$. Figure 5b corresponds to projecting the wave function on the subspace where the hole is absent from the given plaquette. In this case, we apply a corresponding four spins cyclic permutation and calculate the overlap with the ground state. As expected, $\varphi_{\rm eff}$ is zero for the fully polarized ferromagnetic state. When the total spin reaches its minimal value $S = 1/2$, the spins twist in a way which provides a rather good cancellation of the external flux. However, this matching is not as good when the hole is not on the given plaquette and when φ/φ_0 is large. While the three and four site paths are note exactly the same, such a trend is sensible, since we expect the constraint on the spin wave function to be the strongest in the vicinity of the hole. We should also emphasize that these expectation values of spin permutation operators are related to the spin chirality in the following way. Let us consider a 4 sites ring with spins S_1, S_2, S_3, S_4, and denote by P_{ij} the permutation operator for spins i and j. A three spin cyclic permutation P_3 is given by $\mathrm{P}_3 = \mathrm{P}_{12}\mathrm{P}_{23}$ and a four spin permutation P_4 by $\mathrm{P}_4 = \mathrm{P}_{12}\mathrm{P}_{23}\mathrm{P}_{34}$. It can be shown [17]:

$$\mathrm{P}_3 - \mathrm{P}_3^* = -4i\, S_1 \cdot (S_2 \times S_3) \tag{2}$$

$$\mathrm{P}_4 - \mathrm{P}_4^* = -2i\,\{S_1 \cdot (S_2 \times S_3) + S_2 \cdot (S_3 \times S_4) + S_3 \cdot (S_4 \times S_1) + S_4 \cdot (S_1 \times S_2)\}\,. \tag{3}$$

So a finite chirality, defined by $\langle S_1 \cdot (S_2 \times S_3)\rangle \neq 0$ for instance implies that $\varphi_{\rm fic}/\varphi_0$ is not integer nor half integer. The results of figure 5 indicate a finite spin chirality in the ground state expected for $\varphi/\varphi_0 = 1/2$ and the vicinity of $\varphi = 0$. This is consistent with the fact that

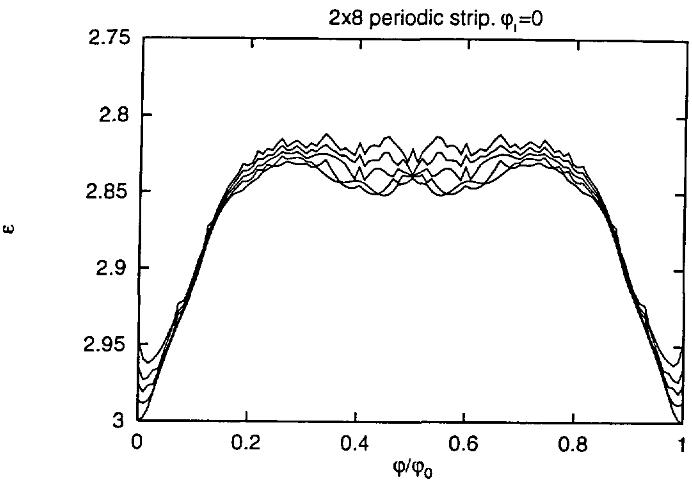

(b)

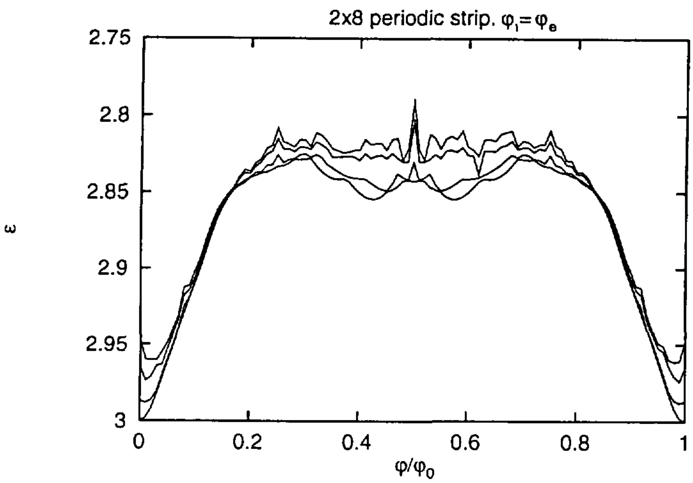

(c)

Fig. 2. — *(continued)*

$\varphi/\varphi_0 = 1/2$ and $\varphi/\varphi = 1/2$ are the only values for which the Hamiltonian (1) does not break time reversal symmetry. Furthermore, finite chirality implies a non-coplanar spin configuration in general. This non coplanarity appears very naturally in a mean field semi classical picture, where spins are assumed to be mutually uncorrelated and pointing in different directions, thus defining a classical unit vector field $\mathbf{n}(i)$ on each site i. With such an hypothesis, the contribution of the spin background to the total phase seen by the hole during its motion around a closed path is half of the solid angle spanned by the vector field $\mathbf{n}(i)$ on the unit sphere when i goes along the path [6]. Our exact diagonalizations suggest that such a semi-classical mean field picture predicts the right variation of the spin chirality as a function of the external flux. However, it has been shown that a class of wave functions leads to a strong

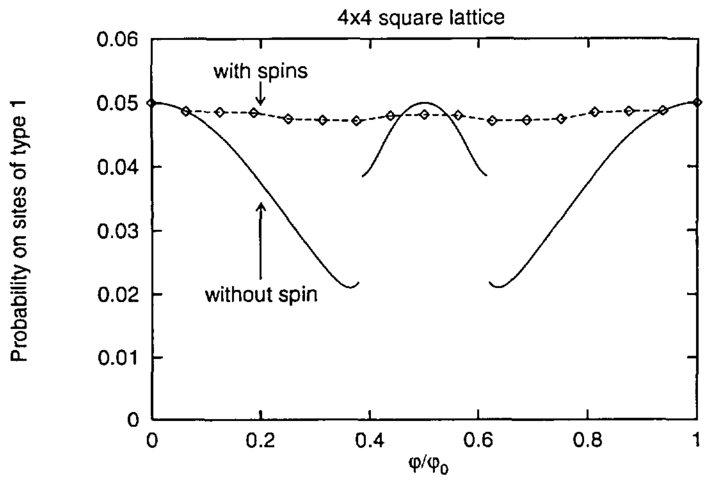

(a)

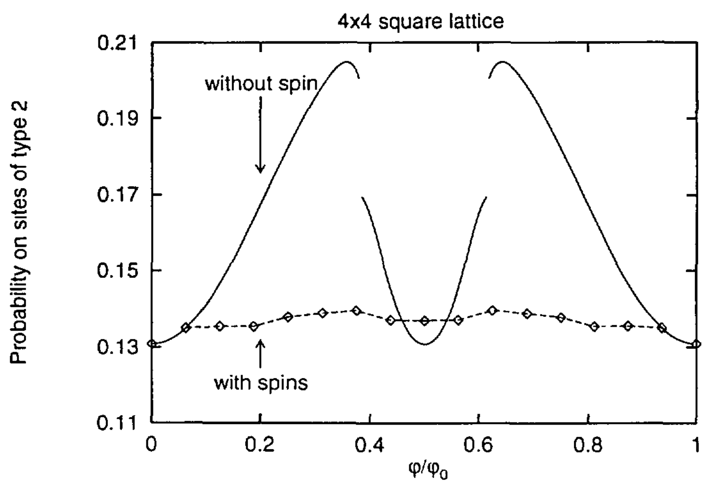

(b)

Fig. 3. — Probability of presence for the hole on different sites in the ground state. a) 4×4 square lattice for sites of type 1 (see Fig. 1b). "With spins" corresponds to the full Hilbert space and "Without spin" to the maximally polarized state, equivalent to a single spinless particle. b) Same as previous case, for sites of type 2. c) 2×8 strip with $\varphi_{\rm i} = \varphi_{\rm e} = \varphi$, for sites on the internam ring. d) 2×8 strip with $\varphi_{\rm i} = 0$ for sites on the internal. Note that the magnification on the y axis is much larger for case c) and d) than for a) and b).

reduction of the modulus of the hopping amplitude, eventhough its phase can be tuned to the right value. It would be of course interesting to know if we can reproduce the ground state energy at finite flux, using a semi-classical static spin background. It is not so straightforward, since it requires an optimization over all the associated unit vector fields $\mathbf{n}(i)$ on the lattice. We haven't attempted this yet, since we suspect that the large finite twist could lead to a too

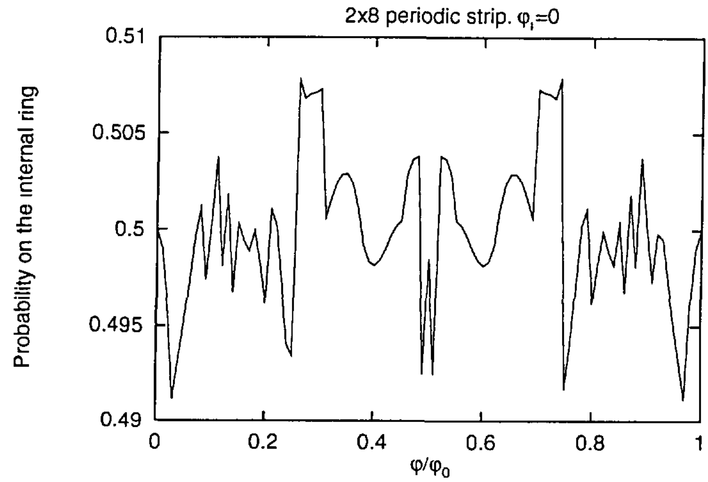

(c)

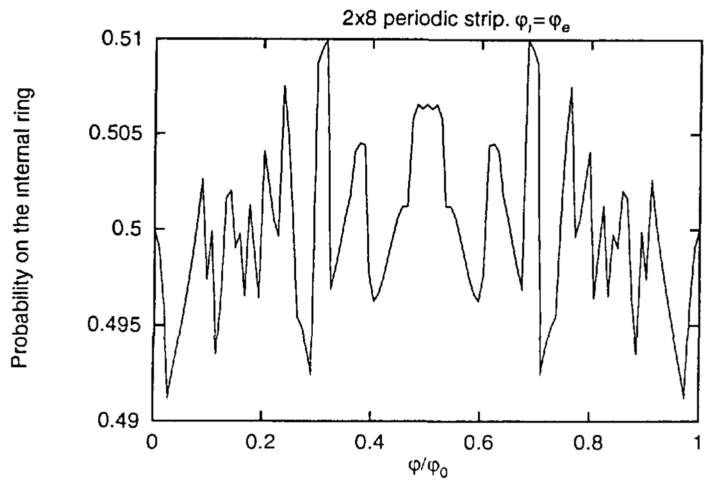

(d)

Fig. 3. — *(continued)*

small absolute value of the hopping amplitude. In principle, those semi-classical states are not eigenstates of the total spin. However, it is always possible to project them onto the subspace with the small value of the total spin. It would be interesting to optimize the overlap between such a state and the actual ground state, to get a better understanding of the physical nature of this ground state.

In this paper, we also report some results on an *a priori* different class of variational wave functions. Rather than starting from a semi-classical picture, which is well adapted when the **n** field varies only on very large length scales (i.e. when $\varphi/\varphi_0 \ll 1$), our trial states definitely contain strong quantum fluctuations. The idea is that the spin part of the wave function should provide a source of fictitious flux acting on the hopping of the hole. Let us denote by x the

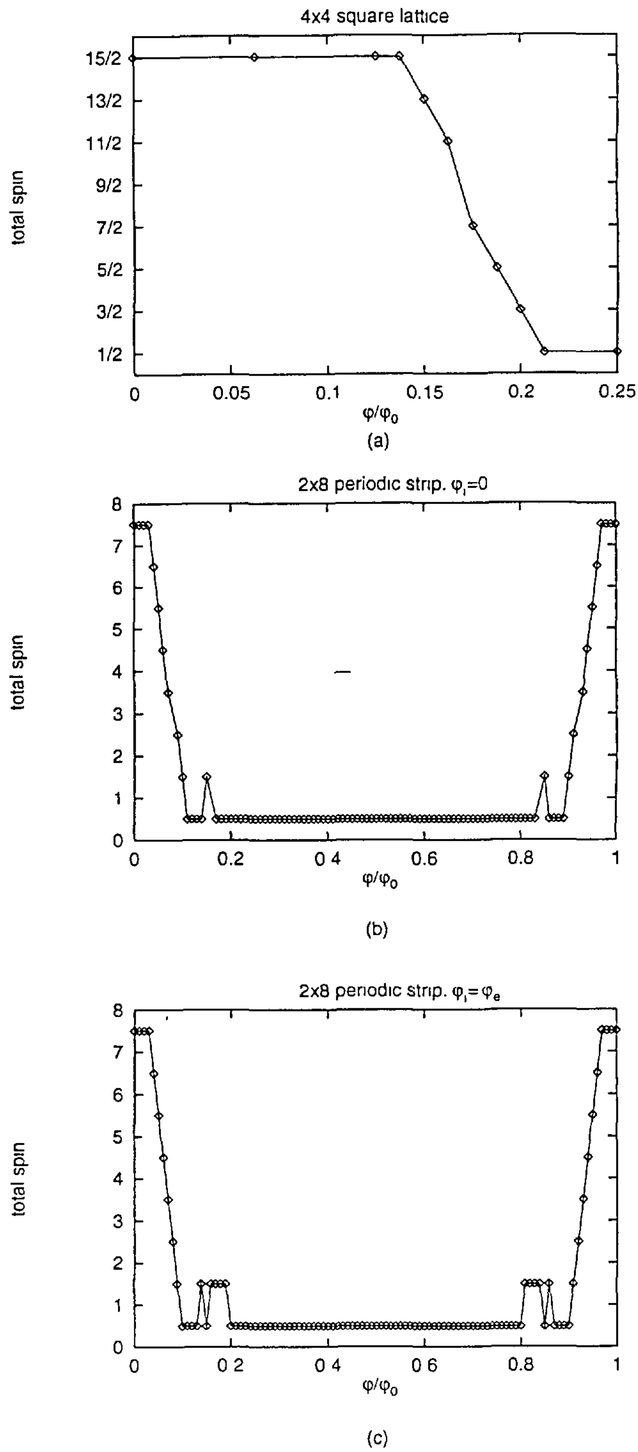

Fig. 4. — Total spin of the ground state *versus* φ. a) square lattice. b) 2×8 strip for $\varphi_{\rm i} = \varphi_{\rm e} = \varphi$. c) 2×8 strip for $\varphi_{\rm i} = 0$ and $\varphi_{\rm e} = \varphi$.

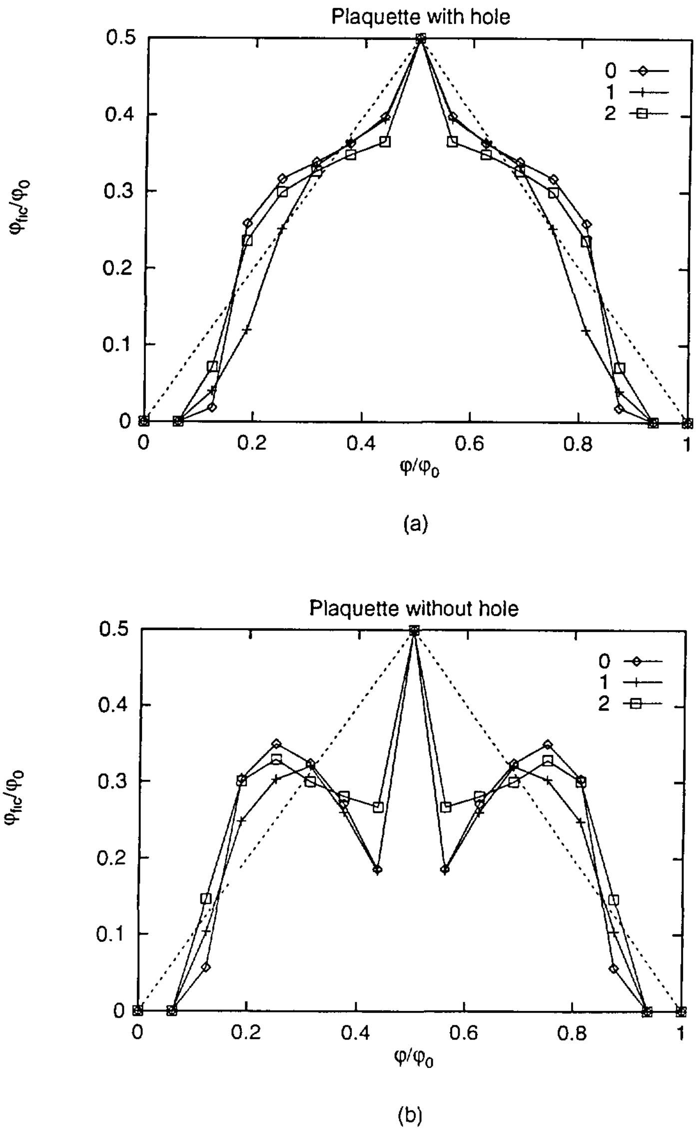

Fig. 5. — Fictitious flux per plaquette as defined in text for the square cluster, for the three types of plaquettes (see Fig. 1a). a) Plaquette with the hole located on it. b) Plaquette without hole. In both case a) and case b) and for = 0.5, a degeneracy of the ground statelead to a values slightly different from 0.5. The discrepency has been corrected by hand.

position of the hole on the lattice, and by y_1, y_2, . , y_n the positions of the n down spins. We investigated wave functions of the form:

$$\Psi\left(x,\ y_1,..,\ y_n\right)=g(x)\prod_{p=1}^{n}\exp\left\{i\theta\left(x,\ y_p\right)\right\}\Phi_{\mathrm{spin}}^{(x)}\left(y_1,..,\ y_n\right). \tag{4}$$

where $\theta(x,\ y)$ is the polar angle of site x with the origin at site y. This wave function binds a fictitious flux tube to each down spin. $\Phi_{\text{spin}}(y_1, .., y_n)$ is a spin wave function and $\Phi^{(x)}_{\text{spin}}$ denotes its restriction to the allowed states with the hole at site x, to values of $y_i \neq x$. We assume $\Phi^{(x)}_{\text{spin}}$ to be normalized, ie:

$$\sum_{\substack{y_1 < y_2 < \quad < y_n \\ y_i \neq x}} \left|\Phi^{(x)}_{\text{spin}}(\mathrm{y}_1, \ . \ , \mathrm{y}_\mathrm{n})\right|^2 = 1. \tag{5}$$

$g(x)$ is interpreted as the hole wave function given this spin background. It depends for instance on the chosen gauge for the A'_{ij}s. So the presence of $g(x)$ is required by gauge invariance. We chose for Φ_{spin} a wave function with a uniform spatial density, with a tunable amount of repulsion between the down spins. More specifically, we assumed a Coulomb gas-Jastrow form:

$$\Phi^{(x)}_{\text{spin}}(y_1, \ . \ , y_\mathrm{n}) = \prod_{m=1}^{n} \exp\left(iQ \cdot y_m - \frac{p}{4\ell^2}|y_m|^2\right) \prod_{1 \leq l < m \leq n} | \, y_m - y_l \, |^p \, / z^{1/2}(x). \tag{6}$$

The length ℓ is chosen to ensure the global neutrality of the corresponding plasma, which leads to:

$$\ell^2 = \frac{L^2}{2\pi n} \tag{7}$$

As this point, we stress that this variational study has been limited to the same square cluster case. We chose the origin of the coordinate system to coincide with the center of the square cluster, and used the lattice spacing as the unit length. $z(x)$ is a normalization factor, determined in order to satisfy equation (5). Unless $p = 0$, it varies with x in general. The wave vectors Q have been either (0, 0) or (π, π) in our trivial wave functions. In all the case we have studied, $Q = (\pi, \pi)$ gives a lower energy. We think this is because each time the hole hops towards a site occupied by a down spin, the phase factor in equation (4) acquires a large additional contribution of π. This interferes destructively with configurations where the hole hops towards an up spin site. Such a negative interference no longer occurs if $Q = (\pi, \pi)$. In what follows, this value of Q has been assumed.

For given values of Q, p, n and φ, we minimize the expectation value of H by adjusting the hole wave function $g(x)$. This is equivalent to an effective one particle tight binding problem since

$$\langle \mathrm{H} \rangle = -\sum_{\langle ij \rangle} t_{ij} \, g^*(x_i) \, g(x_j) + \text{h.c.} \tag{8}$$

with the normalization constraint:

$$\sum_i |g(x_i)|^2 = 1. \tag{9}$$

In equation (8), t_{ij} a complex number given by:

$$t_{ij} = \mathrm{e}^{iA_{ij}} \sum_{\substack{y_1 < \quad < y_n \\ y_m \neq x_j}} \prod_{m=1}^{n} \exp\left\{i\left(\theta(x_j, \, y_m) - \theta(x_i, \, y'_m)\right)\right\} \Phi^{(x_i)^*}_{\text{spin}}(\{y'\}) \Phi^{(x_j)}_{\text{spin}}(\{y\}) \tag{10}$$

In equation (10), the sum runs over spin configurations $\{y\}$ corresponding to the hole located at site j. The spin configurations $\{y'\}$ is defined from $\{y\}$ after the hole has moved from j to i. From Cauchy Schwarz inequality, we have $|t_{ij}| < 1$. Quite generally, we can write:

$$t_{ij} = |t_{ij}| \, \exp\left\{i\left(A_{ij} + a^{\text{fic}}_{ij}\right)\right\} = |t_{ij}| \, \exp\left\{a^{\text{eff}}_{ij}\right\} \tag{11}$$

$a_{ij}^{\rm fic}$ is the fictitious vector potential generated by the spin background. We expect the total fictitious flux through the system to be $n\varphi_0$ in absolute value. Figure 6 shows the variational energy for $p = 2$, and several values of n. The value $p = 2$ seems to provide the best variational states in the class described by equation (6). The main feature is the multiple crossings of the series of curves. As a result, the variational ground state energy corresponds to the lower envelope of this family of curves. In general, for a given value of n, the energy as a function of φ/φ_0 begins to decrease, up to the point corresponding to a vanishing effective flux. A consequence of this series of crossings, is a strong reduction of the amplitude of variation of the variational energy as a function of the external flux. However, the absolute value of the energy is quite above the actual value from exact diagonalization. Furthermore, the variational method overestimates the total spin of the ground state by quite a large amount. In order to understand the nature of these wave functions, it is helpful to study the effective Hamiltonian defined in equation (10). For each plaquette we define an effective flux from the oriented sum of $a_{ij}^{\rm eff}$'s around the plaquette. The phase modulo 2π is chosen to be in the interval $]-\pi,\ \pi]$. The average effective flux $\langle\varphi\rangle$ is then obtained by averaging over all the oriented plaquettes with an equal weight. The result is plotted in figure 7a. As intuitively expected, the optimal wave function corresponds to approximately minimizing the absolute value of $\langle\varphi\rangle$. We note a systematic bias towards a smaller value of n. This behavior is simply related to the results of figure 7b. This last figure represents the amplitude $\langle t\rangle$ which is the average of $|t_{ij}|$ over all links on the lattice with equal weight. Clearly, increasing the number of spin flips reduces $\langle t\rangle$ quite dramatically, thus favoring the state with smaller n at a fixed value of $|\langle\varphi\rangle|$. We conclude this section by stressing that $p = 2$ seems to be a rather sharp minimum for the trial wave function energy. If p is not close to this value, the curves corresponding to figure 6 do not even cross, due to a stronger reduction of $\langle t\rangle$ as a function of n.

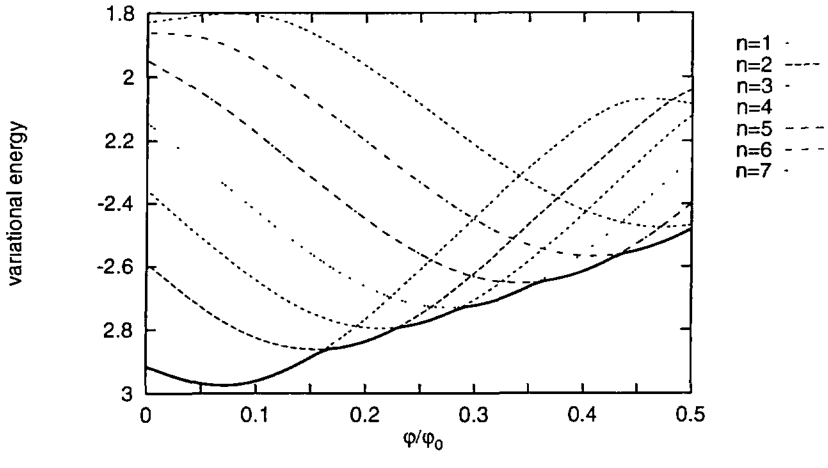

Fig. 6. — Variational energy for the best trial states defined in text on a 4×4 cluster for various values nd of the number of down spins. The thick curve is the lower enveloppe. Note that the fully polarized state ($nd = 0$) has not been included. It is optimal state at small $\frac{\varphi}{\varphi_0}$.

To conclude our report, all the calculations strongly support the picture that the fictitious fields induced by the spin currents (i.e. non coplanar spin configurations) cancel an external

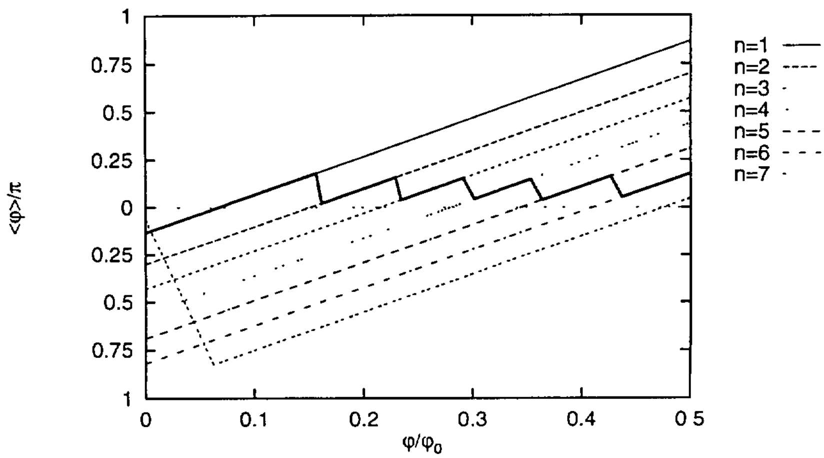

(a)

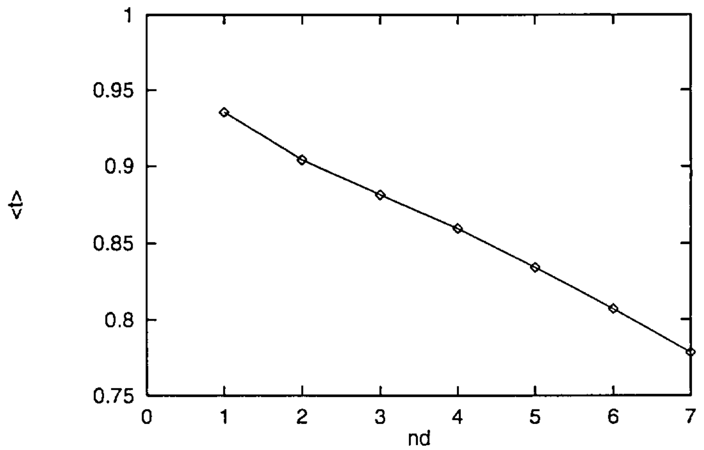

(b)

Fig. 7. — Effective H_{eff} for the hole for the variational wave functions (see Eq. (10)). a) Average effective flux (see Eq. (11)). The thick line represents the actual variational ground state. b) Average hopping amplitude. For each value of φ, nd is chosen so that the variational energy is minimal.

orbital magnetic field. However, it does not seem to be easy to reproduce the rather large effective bandwidth in the presence of a large twist of the spins by simple variational schemes, such as the mean-field semi-classical states of reference [6] or the Jastrow type wave functions discussed here. It seems that the systems take advantage of the exponentially large dimensionality of the subspace corresponding to the minimal value of the total spin. Those who would derive a simple picture for these ground states should concentrate on maximizing the value of $\langle t \rangle$, which appears to be more difficult than simply adjusting the effective flux.

Another important issue is to understand the finite temperature behavior. Some preliminary results of recent Monte Carlo simulations suggest that the fictitious flux φ_{fic} exhibits a very singular behavior at any finite T in the low φ regime, specifically [5], when T is much smaller than the bandwidth, $\left.\frac{\mathrm{d}\varphi_{\mathrm{fic}}}{\mathrm{d}\varphi}\right|_{\varphi=0} \sim \frac{1}{T}$. Extrapolated to $T=0$ this would lead to a finite value of φ_{fic} in the presence of an infinitesimal positive value of φ. This may seem at first glance in contradiction with the results of figure 5. However, taking the $T=0$ limit in the Monte-Carlo simulation of reference [15] amounts to taking the thermodynamic limit. We expect then that the excitation energy of the minimal spin subspace above the Nagoaka state for a single hole at $\varphi=0$ to vanish in that limit. Furthermore, these low spin states may dominate the entropy at any finite temperature. One of the striking results of reference [14] is the observation of a finite chirality of φ_{fic} in the limit of $\varphi \rightarrow 0$ for the minimal value of the total spin. Of course, these states have a finite excitation energy for a finite size system. If they survive in the thermodynamic limit, they may be the way to reconcile finite cluster diagonalizations and finite temperature studies. The idea that low spin states with quite different properties compared to the ferromagnetic state may dominate physical observables at finite T is also suggested in the high T series expansions of reference [10] where, in the absence of external flux, no evidence of ferromagnetism appears at any density of holes.

Acknowledgements.

The work was initiated while R. Rammal was still among us. He provided the impetus and many ideas. His suggestion to study several geometries certainly reflects his taste for a systematic approach in the face of a new problem. We imagine that he would have appreciated figure 6! (see Ref. [18]).

References

[1] NAGOAKA Y., *Phys. Rev.* **147** (1966) 392.
[2] TAKAHASHI M., *J. Phys. Soc. Jpn* **51** (1982) 3475.
[3] RIERA and YOUNG A.P., *Phys. Rev. B* **40** (1989) 5285.
[4] FANG Y., RUCKENSTEIN A., DAGOTTO E. and SCHMITT-RINK S., *Phys. Rev. B* **40** (1989) 7406;
ANGLÈS D'AURIAC J.C., DOUÇOT B., RAMMAL R., *J. Phys.: Cond. Matter* **3** (1991) 3973.
[5] DOUÇOT B. and WEN X.G., *Phys. Rev. B* **40** (1989) 2719.
[6] DOUÇOT B. and RAMMAL R., *Phys. Rev. B* **41** (1990) 9617.
[7] SHASTRY B.S., KRISHNAMURTHY H.R., ANDERSON P.W., *Phys. Rev. B* **41** (1990) 2375.
[8] BASILE and ELSER V., *Phys. Rev. B* **41** (1990) 4842.
[9] VON DER LINDEN W. and EDWARDS D.M., *J. Phys.: Cond. Matter* **3** (1991) 4917.
[10] PUTTIKA W.O., LUCHINI M.V., OGATA M., preprint.
[11] BARBIERI A., RIERA J.A. and YOUNG A.P., *Phys. Rev. B* **41** (1990) 11697.
[12] LIEB E. and WU F., *Phys. Rev. Lett.* **20** (1968) 1445.
[13] IOFFE L.B. and WIEGMANN P.B., *Phys. Rev. Lett.* **65** (1990) 653.
[14] SCHOFIELD A.J., WHEATLEY J.M. and XIANG T., *Phys. Rev. B.* **44** (1991) 8349.
[15] MESHKOV S. and ANGLÈS D'AURIAC, preprint.
[16] FRADKIN E., *Phys. Rev. Lett.* **63** (1989) 322.
[17] WEN X.G., WILCZEK F. and ZEE A., *Phys. Rev. B* **39** (1989) 11413.
[18] RAMMAL R., LUBENSKY T.C. and TOULOUSE G., *Phys. Rev. B* **27** (1983) 2820.